Evaluation of Geomorphological Features of Çoraklı Landslide (Şavşat, Artvin, Türkiye)*

Çoraklı Heyelanının Jeomorfolojik Özelliklerinin Değerlendirilmesi (Şavşat, Artvin, Türkiye)

Ergin CANPOLAT[1] , Onur HALİS[2] , Ferhat KESERCİ[3] , Cihan BAYRAKDAR[2]

[1]Hatay Mustafa Kemal University, Faculty of Arts and Sciences, Department of Geography, Hatay, Türkiye
[2]Istanbul University, Faculty of Arts and Sciences, Department of Geography, Istanbul, Türkiye
[3]Ardahan University, Ardahan Faculty of Humanities and Arts, Department of Geography, Ardahan, Türkiye

ORCID: E.C. 0000-0003-2123-3551; O.H. 0000-0002-0643-2651; F.K. 0000-0002-8653-6177; C.B. 0000-0001-5542-700X

ABSTRACT

This study investigates the landslide area that affects approximately 52 hectares northwest of Çoraklı village center in Şavşat district, Artvin province, from a geomorphological perspective. The area was mapped using topographic maps, UAV-acquired images, orthophotos, and detailed field studies. The study area features Paleogene-aged volcanic sedimentary rocks and Eocene-clastic and carbonate rocks, which have high clay production potential, combined with steep slopes. Meteorological data indicate that this region receives more rainfall than its surroundings, creating favorable conditions for landslide formation. The landslide, occurring at elevations between 1,270 and 1,700 meters, started as a slide in higher areas and progressed as a debris flow toward the valley floor. The area is marked by a prominent main landslide scarp about 60 meters high, forming a crescent shape. The longest section of the landslide flank was 345 meters. The distance between the residential structures in Çoraklı village and the landslide crown was less than 20 meters. Fresh and flow-type mass movements were observed at the toe of the landslide and in nearby areas. The potential for existing landslides in this region underscores the urgent need for measures to be taken in this area of the Çoraklı settlement.
Keywords: Landslide, Natural Disaster, Şavşat

ÖZ

Bu çalışmada, Artvin ili Şavşat ilçesi Çoraklı köyü merkezinin kuzeybatısında yer alan ve yaklaşık 52 hektarlık alanı etkileyen heyelan sahası jeomorfolojik açıdan incelenmiştir. Saha, topografya haritaları, insansız hava aracı (İHA) ile alınan fotoğraflar, ortofoto ve detaylı arazi çalışmaları ile haritalanmıştır. Alanda Paleojen volkano-sedimanter kayaçlar ile Eosen dönemine ait kırıntılı ve karbonatlı kayaçlar yer almaktadır. Sahada kil üretme potansiyeli yüksek olan bu kayaç yapılarına ek olarak yüksek yamaç eğimleri de görülmektedir. Meteorolojik veriler, bu kesimin yakın çevresine göre nispeten daha fazla yağış aldığını da ortaya koymaktadır. Tüm bunlar, sahada heyelan oluşumu için gerekli olan zemini hazırlamıştır. 1170-1700 metre yükselti aralığında gerçekleşmiş olan heyelan, yüksek kesimlerde kayma şeklinde başlayıp, vadi tabanına doğru moloz akması biçiminde ilerlemiştir. Heyelan, yaklaşık 60 metre yüksekliğinde belirgin bir hilal şekilli ana heyelan aynası ile dikkat çekmektedir. Heyelanın sağ ve sol kanat aralığının en uzun kısmı 345 metredir. Çoraklı köyü yerleşim yerini oluşturan mesken ve diğer yapıların taç kısmına en fazla yaklaştıkları kesim ile taç kısmı arasında ise 20 metreden daha kısa bir mesafe vardır. Heyelanın etek kısmında ve yakın çevrede taze ve akma şeklinde kütle hareketi gözlemlenmiştir. Bu bölge ve yakın çevredeki heyelanların potansiyeli, Çoraklı yerleşim yerinde acil tedbirlerin alınması gerekliliğini ortaya koymaktadır.
Anahtar kelimeler: Heyelan, Doğal Afet, Şavşat

1. INTRODUCTION

Landslides, which refer to the movement of a mass of rock, debris, or soil down a slope (Cruden & Varnes, 1996; Varnes, 1984), can sometimes reach the level of a disaster, causing loss of life and property (Gökçe et al., 2008; Görüm & Fidan, 2021). According to EMDAT data, more than 300 fatal landslides occurred between 2003 and 2023, resulting in 17,414 deaths and billions of dollars in material damage (EMDAT, 2024). Due to these characteristics, landslides rank among the top mass movements in the world in terms of the number of incidents and fatalities caused by natural disasters. In recent years, landslides have become more common because of the effects of increasing extreme weather events and human activities, posing a threat to sustainable development in areas with high landslide susceptibility (Fidan et al., 2024). In Türkiye, where slope values and elevations are high, landslides can occur in every geographical region. However, they occur most frequently in the Black Sea Region, especially in the Eastern Black Sea, and lead to significant disasters. Between 1929 and 2019, 389 landslides occurred throughout Türkiye, resulting in the deaths of 1,343 people (Fidan & Görüm, 2020).

Landslide damages can be categorized as direct impacts and environmental effects. Direct damage affects human health, homes, properties, agriculture, infrastructure, dams, and industrial facilities. Environmental impacts include morphological changes, destruction of forests and grasslands, disruption of stream ecosystems, harm to wildlife, and water quality deterioration. Additionally, landslides can cause social and economic losses, insurance challenges, increased real estate costs, tsunamis, and coastal damage (Schuster & Highland, 2007; Alimohammadlou et al., 2013).

When the studies conducted to date are evaluated, it is understood that various types of classifications have been made for landslides (Cruden & Varnes, 1996; Erinç, 2002). However, the most common classification is that by Varnes (1978) and Cruden and Varnes (1996), which classifies landslides based on material type and movement (Figure 1).

A classification method for landslides is based on the type of movement. This classification includes falling, toppling, sliding, spreading, flowing, and complex movements. Each type of movement is influenced by various factors such as lithology, structural conditions, and topographic features (Crunden & Varnes, 1996; Dai et al., 2002). Falling movements typically occur on slopes with angles ranging from 48° to 70°. The falling movement is primarily influenced by lithological and structural factors. High-angle slope gradients make material susceptible to rocks or debris detaching from the slope and freely descending or falling down the slope due to gravity (Gutiérrez & Gutiérrez, 2016).

Although it varies in different areas, sliding movements mostly occur on slopes with a slope ranging from 18° to 40°. The sliding movement depends on a combination of factors such as NDVI (Normalized Difference Vegetation Index), proximity to roads, slope gradient, heavy rainfall, snowmelt water (Niraj et al., 2023; Moazzam et al., 2020, Cihangir et al., 2018). Sliding refers to the downward movement of material along a defined failure surface (planar or rotational), but other landslide subtypes exist, such as falls (vertical detachment), topples (rotational overturning), flows (fluid-like movement), creeps (slow deformation), and complex movements (combinations of types). These highlight the diversity of landslide mechanisms beyond sliding.
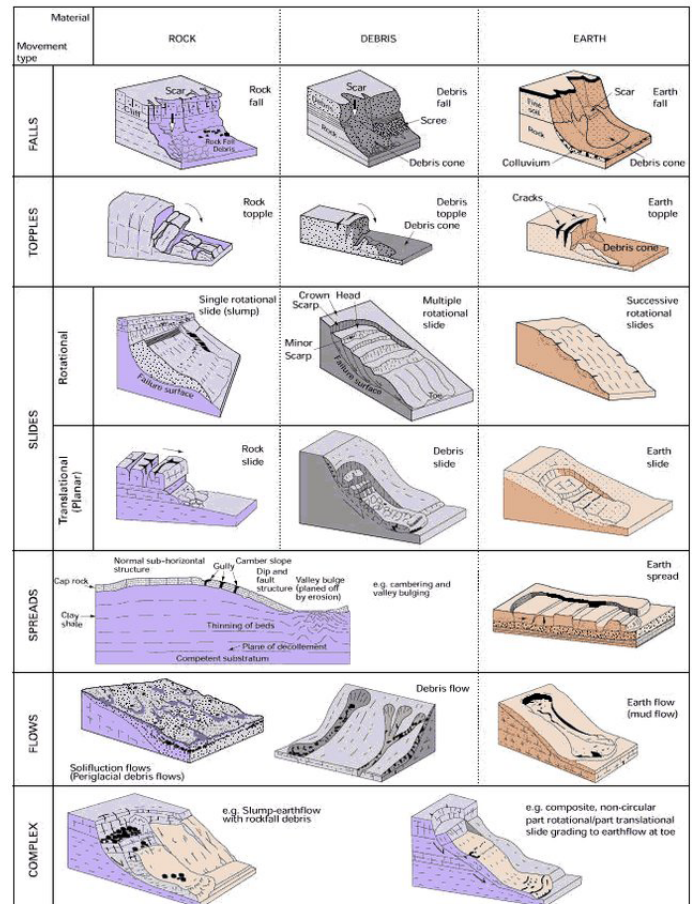

Figure 1: Classification of landslides by Varnes (1978) and Cruden and Varnes, 1996. Allen et al., 2000.

Factors influencing sliding movements include elevation, soil type, distance to roads, distance to rivers, lithological and structural conditions, slope gradient, Topographic Wetness Index (TWI), curvature, land use, NDVI, and aspect features (Xia et al., 2023; Makonya & Zahor, 2023). The effect of vegetation on landslides can be either triggering or mitigating, depending on the slope, soil type, root depth and hydrological conditions where water is available. The NDVI index can be used to assess plant presence and health. Roads and road construction works can change the drainage pattern in the area, create new slopes and thus disrupt the slope stability. These characteristics can also increase the probability of sliding on the slope. The slope gradient plays a primary role in both falling and sliding motions. An excessive increase in slope gradients increases the potential for falling; however, moderate slope gradients increase the potential for sliding. Although all these factors affect mass movements in the form of flow, particularly rapid snowmelt and intense and heavy rainfall, they have a high potential to trigger flow-type landslides (Amarasinghe et al., 2024).

Landslides are also classified based on their activity status. According to WP/WLI (1993), active landslides are those that are currently moving or are likely to move in the near future. Inactive (Dormant) landslides are those that are not currently moving but could become active under appropriate conditions. Relict landslides are those that have stabilized and are unlikely to move in the current geological period.

Active, inactive, and relict landslides are frequently observed in Türkiye, particularly on steep slopes and fault zones (Gökçe et al., 2008). In addition, numerous landslides occur in lithological units rich in clay minerals, such as turbiditic sandstone and marl, as well as in flysch formations and contact points between different lithological units (Taşdemiroğlu, 1970; Kopar, 2011; Ertek, 1999; Bayrakdar et al., 2020). Landslides triggered by excessive rainfall (Reis et al., 2008; Cihangir et al., 2018) and earthquakes (Görüm et al., 2023) are also commonly encountered. Furthermore, landslides triggered by human activities are frequently observed on highways (Doğu et al., 1989; Erginal & Bayrakdar, 2005; Aykır, 2023; Bozdoğan & Canpolat, 2022), in mining operations (Erginal et al., 2008; Eker et al., 2024), and in residential areas (Türkeş et al., 2006).

In the high-slope and rainfall-abundant regions of the Eastern Black Sea, where volcanic lithological material has a high potential for clay production, landslides frequently occur, leading to material and non-material losses (Gökçe at al., 2008). This study aims to geomorphologically examine the landslide affecting an area of approximately 52 hectares, located north of the center of Çoraklı village in the Şavşat district of Artvin province, which poses a threat to the village settlement. The primary objectives are to reveal the dimensions of the landslide and to investigate the changes it has caused in the surrounding area.

2. MATERIALS AND METHODS

Various base datasets were used to evaluate the geomorphological characteristics of the landslide area. The main data used include a 12-meter resolution AlosPalsar Digital Elevation Model (DEM) as topographic data, a 1:5000 scale DEM obtained from the General Directorate of Mapping (HGM), and a DEM with a resolution of more than 10 cm generated from the point cloud of images captured by the DJI Mavic 3 Enterprise.

To explain the lithological units in the study area and their characteristics, geological data were derived from 1:100,000 (F-47, F-48) and 1:500,000 (Kars) scale geological map sheets and related reports from the General Directorate of Mineral Research and Exploration (MTA).

Climatic data obtained from the General Directorate of Meteorology (MGM) were used to evaluate the control of the climatic features of the landslide. The temperature, precipitation, and wind characteristics were primarily analyzed using data from MGM. In addition, to evaluate the precipitation characteristics of the studied area using other sources, long-term data from WorldClim, CHELSA, and CHIRPS were also considered. Monthly bulletin data were obtained from MGM for the study area and its surroundings. Using these values, a precipitation distribution map for the study area was prepared using the IDW interpolation method. For the section of the Çoraklı Landslide and its surroundings, WorldClim 2.1 (30 arc seconds) precipitation data were preferred for comparison with MGM station data. WorldClim 2.1 (30 arc seconds) is a global model dataset that integrates monthly climate data from 1970-2000 at approximately 1 km² resolution for terrestrial areas worldwide (Fick & Hijmans, 2017). In addition to weather station data, satellite-based variables, such as maximum and minimum land surface temperatures obtained from the MODIS satellite platform, were also used to create the WorldClim dataset (Fick & Hijmans, 2017). Another global climate model used for comparison is CHELSA. The CHELSA dataset is a downscaled high-resolution version of temperature and precipitation predictions from the ERA-Interim climate reanalysis model output at 30-arc-second (1 km²) resolution (Karger et al., 2017).

The precipitation algorithm includes orographic predictors such as wind field, valley position, and boundary layer height, followed by bias correction (Karger et al., 2017). The obtained data include monthly precipitation data for the years 1979-2013.

The last global climate model used for comparison was the Climate Hazards group's Infrared Precipitation with Stations (CHIRPS). The climate model is primarily based on annual precipitation, soil moisture, and runoff modeling from 1981 to 2014. The CHIRPS dataset creates a global climate model using data sources such as the Tropical Rainfall Measuring Mission Multi-satellite Precipitation Analysis version 7 (TMPA 3B42 v7) and the Global Historical Climate Network (GHCN) (Funk et al., 2015). Additionally, CHIRPS data are generated using the Climate Hazards Precipitation Climatology (CHPclim) dataset, which provides a global 0.05° monthly precipitation climatology (Funk et al., 2015).

These datasets were used to support long-term precipitation forecasts and analyses (Funk et al., 2015). All three global climate models combine meteorological station data with satellite imagery to produce model outputs. However, due to differences in the number of meteorological stations used, the resolution of satellite and reanalysis data, and bias corrections, noticeable differences, especially in precipitation data, can be observed between the models.

To assess the impact of land use in the study area on landslides and the potential effects of landslides, the 2018 dataset from the "Coordination of Information on the Environment" (CORINE) was used. This dataset was created by the European Environment Agency and was designed according to 44 land-use classes. The European Environment Agency aims to identify changes in the natural environment in each participating country using CORINE land use data and to promote more rational management of natural resources by creating a standardized database for this purpose. It also contributes to the development of environmental policies for member countries (Ministry of Agriculture and Forestry of Türkiye, 2024).

To assess the health and density of the vegetation, an NDVI (Normalized Difference Vegetation Index) analysis was conducted. For the study area, an NDVI map was produced using the 4 (Red) and 5 (Near Infrared) bands of the Landsat 9 satellite from August 27, 2023, late in the summer. The index values ranged from 1 to +1, with high positive values indicating dense vegetation and negative values representing barren rock and soil surfaces and settlement areas (Tucker, 1979; Sellers, 1985).

The study also includes landslide susceptibility maps prepared under the Artvin Disaster Risk Reduction System (IRAP). The maps produced within the IRAP framework were created using the Logistic Regression Model in ARAS, considering parameters such as lithology, elevation, slope, aspect, curvature, land cover, and proximity to streams. Futhermore, landslide maps created by Duman et al. (2009) at the MTA for the research area and its surroundings were also utilized.

During the study, the Agisoft Metashape Professional, ArcGIS Pro, QGIS, SAGA, and OpenJump software packages were used. Agisoft software was used to process the images acquired by the drone to generate point clouds, orthophotos, and 3D modeling. Spatial data evaluations for the study area, including slope, aspect, elevation features, and profile analyses of the landslide site, were carried out using ArcGIS Pro 3.2 software with the help of high-resolution DEM data. To create the geomorphology map, a Red Relief map was generated from the DEM data using QGIS and SAGA software (Chiba et al., 2008; Özpolat et al., 2020; Canpolat, 2021). The resulting base morphometric data, along with orthophotos and fieldwork findings, were used to produce a geomorphology map of the landslide site.

To obtain the slope-curvature values and characteristics of the landslide area, profile analyses were conducted. Topographic profiles were extracted using DEM data to geomorphologically assess the landslide area. A total of 6 profile line analyses were conducted, including 2 in the northwest-southeast direction and 4 in the southwest-northeast direction. The normalized stream profile proposed by Perez-Pena et al. (2017) was also used in this study. This analysis is a tool used to measure the long-term or short-term evolution of terrain. The proposed method combines stream and digital elevation data to generate normalized longitudinal river profiles and provides information on the concavity (CT), maximum concavity (Cmax), and length at maximum concavity (Lmax) (Perez-Pena et al., 2017). The profiles were generated using the NProfiler plugin on ArcMap 10.8.

For the 2D (two-dimensional) analysis of the landslide area, OpenJump GIS software was used. This software is open-source and accessible and can include and run plugins. The PolyMorph-2D plugin was used for 2D dimensional analyses. This plugin allows basic calculations of natural or human-made vector structures, such as location, length, width, perimeter, radius, area, and orientation. It also calculates parameters like axis

Figure 2: Location of study area.

ratios, ellipticity, circularity, compactness, dispersion, complexity, elongation, regularity, convexity, concavity, rigidity, rectangularity, roundness, and sphericity, and adds these values to the polygon's attribute table. These new parameters remain unchanged if the polygon's position and scale information are altered (Güler et al., 2021).

In this study, the calculations of Polygon Area (m2), Volume of Moving Material (m3), Polygon Length (PPOL), Major Axis Length (LPOL) (L), Minor Axis Length (WPOL) (W), Angle from North to East (0°-179°), Minimum Enclosed Box Area within the Polygon (AMEB), Convex Hull Area, Minimum Bounding Circle Radius within the Polygon (RMCC), and Maximum Inscribed Circle Area within the Polygon (AMIC) were conducted according to Güler et al., 2021. Additionally, calculations for the width-length ratio (W/L) (WTLR) (Zingg, 1935), Ellipse Factor (L_W)/(L+W) (ELLF) (Buendía et al., 2002), Elongation Factor (4 A /JI)0.5 / L (ELOF) (Schumm, 1956), and Convexity CONV (PCHU /P) (CONC) (Glasbey & Horgan, 1995) were performed as outlined in the study by Güler et al. (2021).

2.1. Study Area

The study area is located to the northwest of the center of Çoraklı village, which is an administrative part of Şavşat district, Artvin province. It is situated between the geographic coordinates of 41°21'30" N – 41°23'00" N latitude and 42°20'30" E - 42°21'45" E longitude. The landslide area, which occurred on the slope east of a stream valley that flows into the İmerhav Stream, was situated at elevations between 1170 and 1700 m (Figure 2) and total landslide of the study area is 519,378.65 m².

3. RESULTS

3.1. Geological Characteristics

The area where the landslide occurred is located on a slope of a valley extending in a northeast-southwest direction in the Eastern Black Sea Mountains, at an elevation range of 1170-1700 meters. The landslide took place in a section where lithological units of different types are in contact with each other. While Eocene clastic and carbonate rocks are present in the landslide area, the most common lithological units in the immediate vicinity are Eocene volcanic-sedimentary rocks and Eocene andesites (Yılmaz et al., 1998) (Figure 3). In this rock group, clastic and carbonate structures are found in layers that do not exceed 30 cm in thickness. The layers dip in a NW-SE direction. The surface layers are generally beige, while the lower layers are gray (Photo 1a). The change in lithological units on the slope where the Çoraklı landslide occurred, particularly in the 1500–1600 m altitude range, facilitates an increase in the slope in this section and causes the landslide to transform from a sliding type to a flow-type landslide.

Slope instability on the landslide's slip and flow zones has led to the formation of small and large water ponds due to the presence of adjacent slopes with concave and convex curvature characteristics (Photo 1b). The impermeability of the lithological units and their saturation with water indicate that the materials derived from the bedrock have a high potential for clay production. Indeed, the presence of clay that absorbs water, becomes heavier, increases in volume, and becomes slippery is an important factor in landslide formation. Although no direct analysis of clay production has been conducted, the mineralogical characteristics of the rocks and the weathering observations in the field support this interpretation. Additionally, the relevant literature indicates that similar rocks undergo weathering processes that lead to clay formation. However, further analyses are needed to confirm this more definitively.
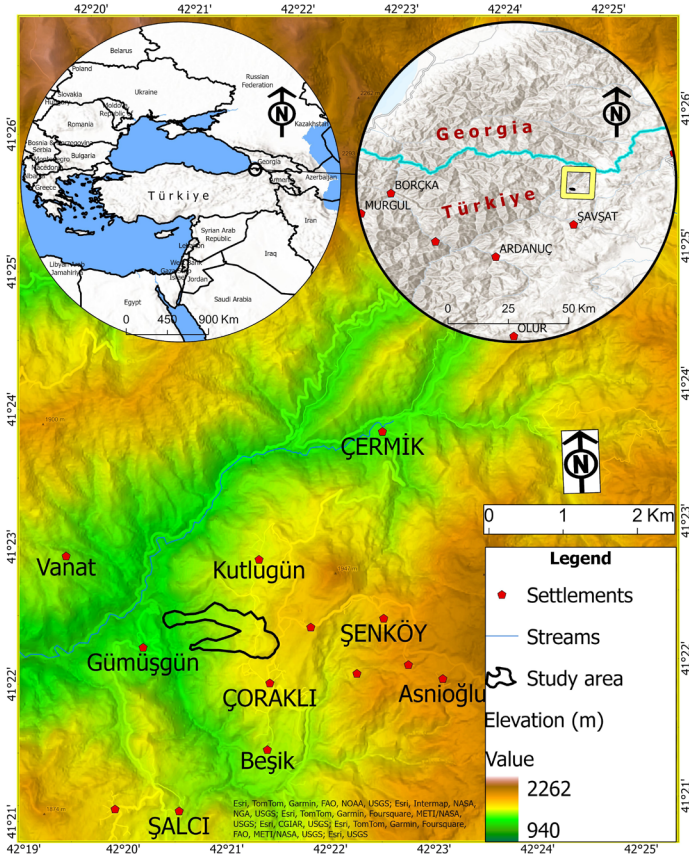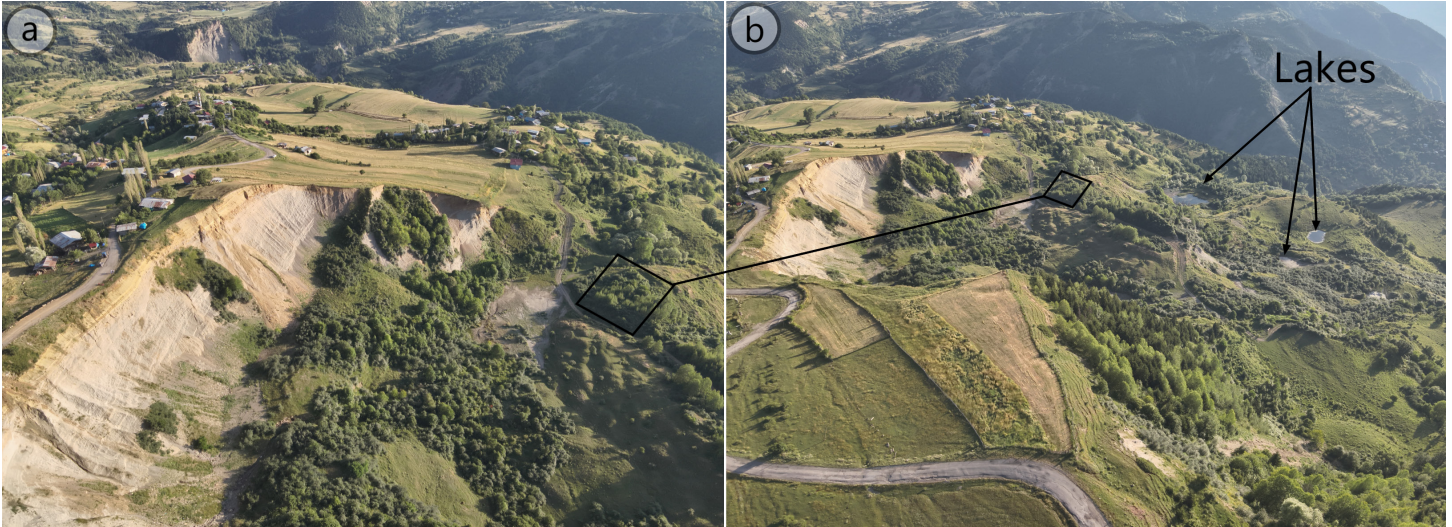
Photo 1. a. Landslide scarp, b. Lakes formed in the landslide area.

Despite the absence of fault markings in the geological maps produced by the MTA for the landslide area, the presence of volcanic lithology in the area, thermal fields with hot springs (36°C) located immediately north of the area (MTA, 2010), and signs such as slope fractures and the orientation of the valleys serve as evidence of fault presence in the area (Figure 3).

The landslide susceptibility map produced by the Artvin Governorship as part of the IRAP studies was classified using the natural breaks (Jenks) method, resulting in five categories of landslide hazard zones. These categories are defined as follows: 1-very low, 2-low, 3-moderate, 4-high, and 5-very high hazard. According to this classification, the area around Şavşat district center and the section where the Çoraklı landslide site is located
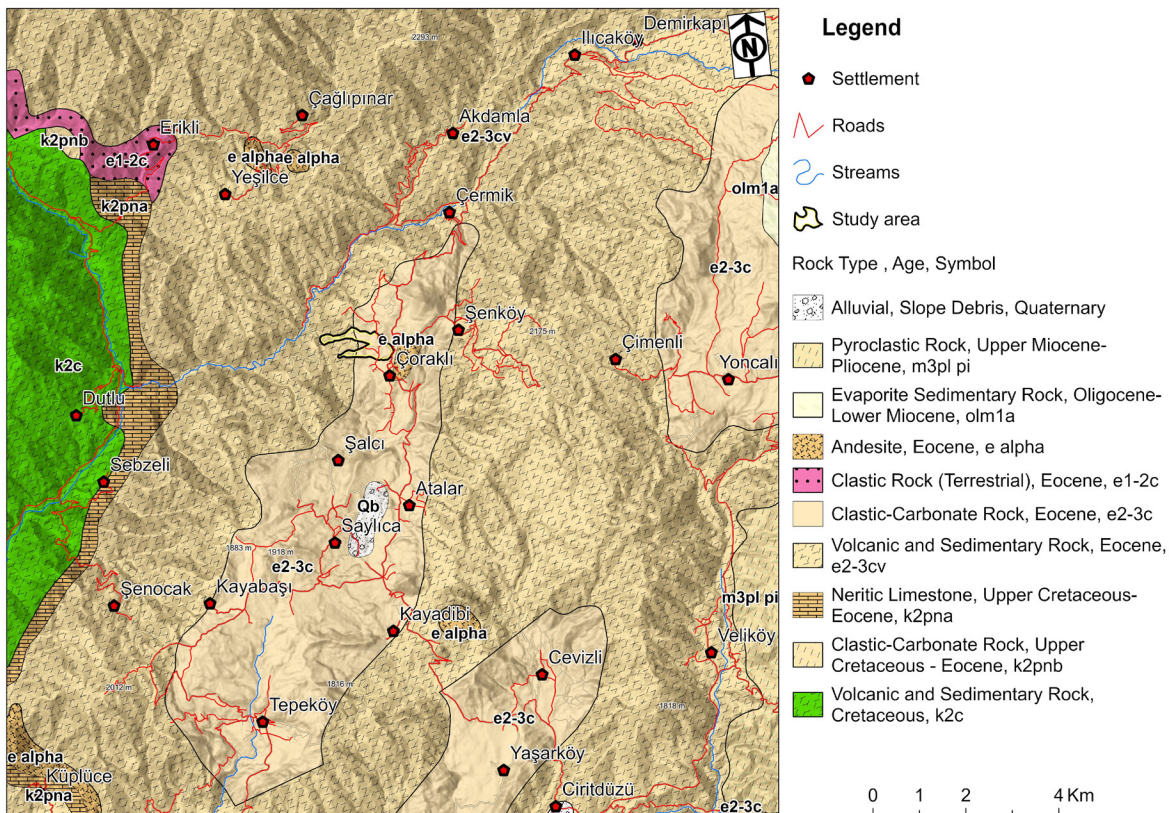

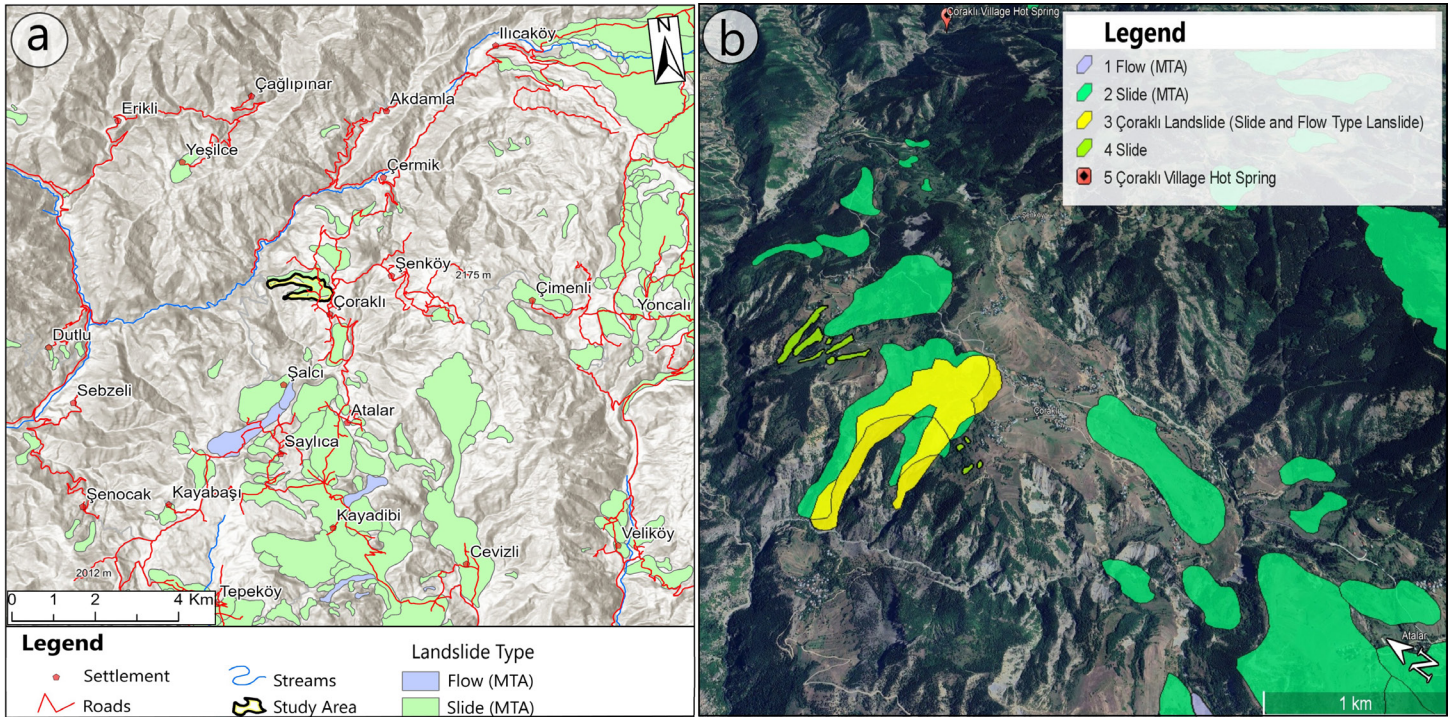**Figure 3.** Geological map of the study area (based on MTA, 1998).

Figure 4. a. Mapped landslides in the study area and its surroundings according to MTA, Duman et al, 2009. b. Landslides according to MTA, Duman et al, 2009 and this study.

fall into the "very high hazard" category. Additionally, numerous landslide sites in and around the Çoraklı landslide area have been mapped according to Duman et al., 2009 (Figure 4 a). As these studies and our assessments indicate, the area around Çoraklı village is highly susceptible to landslides. In our studies and analysis, many recent slide traces were detected in the field (Figure 4 b). Although the lithological units in the field are generally similar, factors such as aspect, steep slopes, the orientation of rock layers, precipitation, snowmelt, and land use play a significant role in the formation of these landslides. While the area is predominantly characterized by slide-type landslides, flow-type landslides are also observed in certain locations.

3.2. Climate Characteristics

When evaluating the climate characteristics of the study area primarily using data from the Şavşat meteorological station, it is evident that the area is located in a transition zone between the mild effects of the Black Sea climate and the distinct features of the continental climate. The winter is particularly long and harsh. The snowfall starts in early November and continues until mid-April. During this period, the region is generally covered with snow, and the cold and snowy characteristics of winter are a general climatic feature of the region. According to the more distant Artvin Meteorological Station, the annual precipitation was 691.6 mm and the temperature was 12.4°C (Figure 5a).

According to data from the Şavşat Station (elevation 1125 m) recorded between 2013 and 2022, the annual average temperature was 10.3°C, and the annual total precipitation average was 713 mm (Figure 5 b). The predominant wind direction at the station was the ESE (Figure 5 c). The average wind speed was around 1 m/s. According to two years of data (2021-2022) from the Yavuzköy station located southeast of the Şavşat district center, the annual average temperature was 7.5°C, and the annual total precipitation average was 1030 mm. According to three years of data from the Meydancık meteorological station located 10 km NW of the landslide area, the temperature was 9.7°C, and the annual precipitation average was 683 mm. In terms of the temperature in the region, average values are below 0°C in December, January, February, and March. The highest precipitation was observed in spring.

To determine precipitation values in the study area, various data sources, including the CHIRPS, WorldClim, and MGM datasets, were used. Monthly precipitation values from the WorldClim and CHELSA climate models were obtained and used to calculate annual total precipitation values for comparison with the MGM station data. The CHIRPS climate model data were downloaded for Türkiye using Google Earth Engine coding methods and scaled for the study area and its vicinity. To enable the combined evaluation of data from different categories, all data were converted into raster data systems with the same level
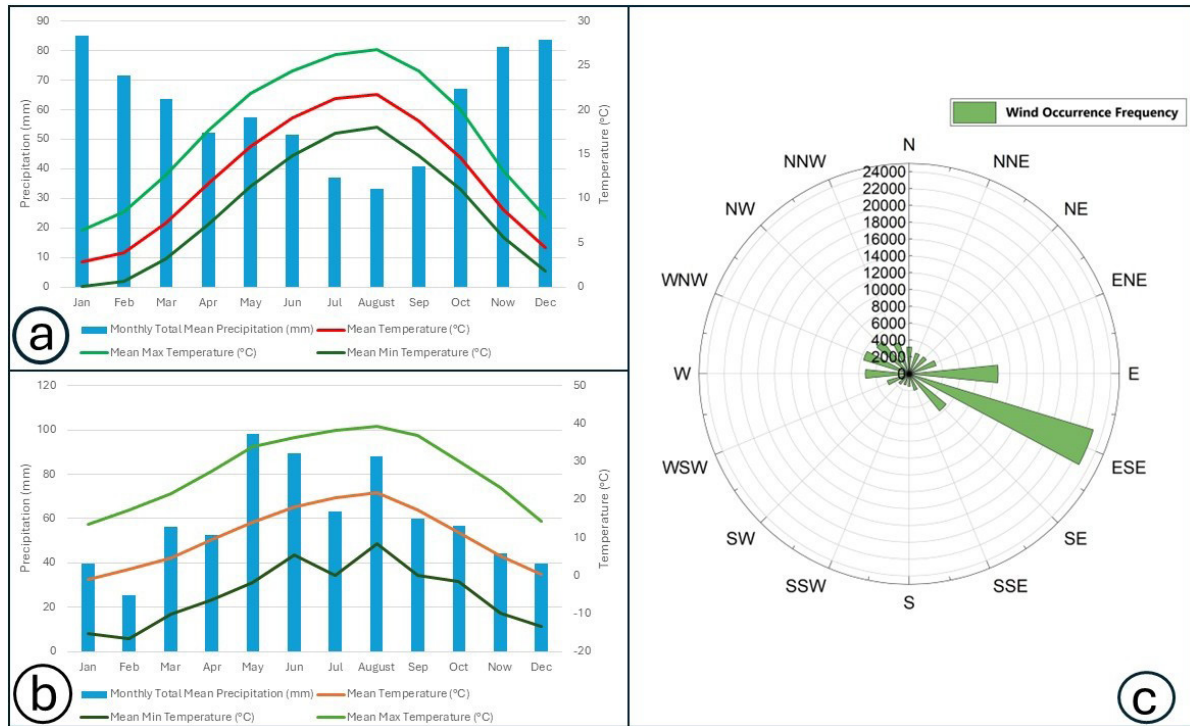
Figure 5. a. Climate graph of the Artvin meteorological station (data from 1949to2023); b. Figure 1. Climate graph of the Şavşat meteorological station (data from 2013 to 2023); c. Wind rose of the Şavşat meteorological station (data from 2013to2023).
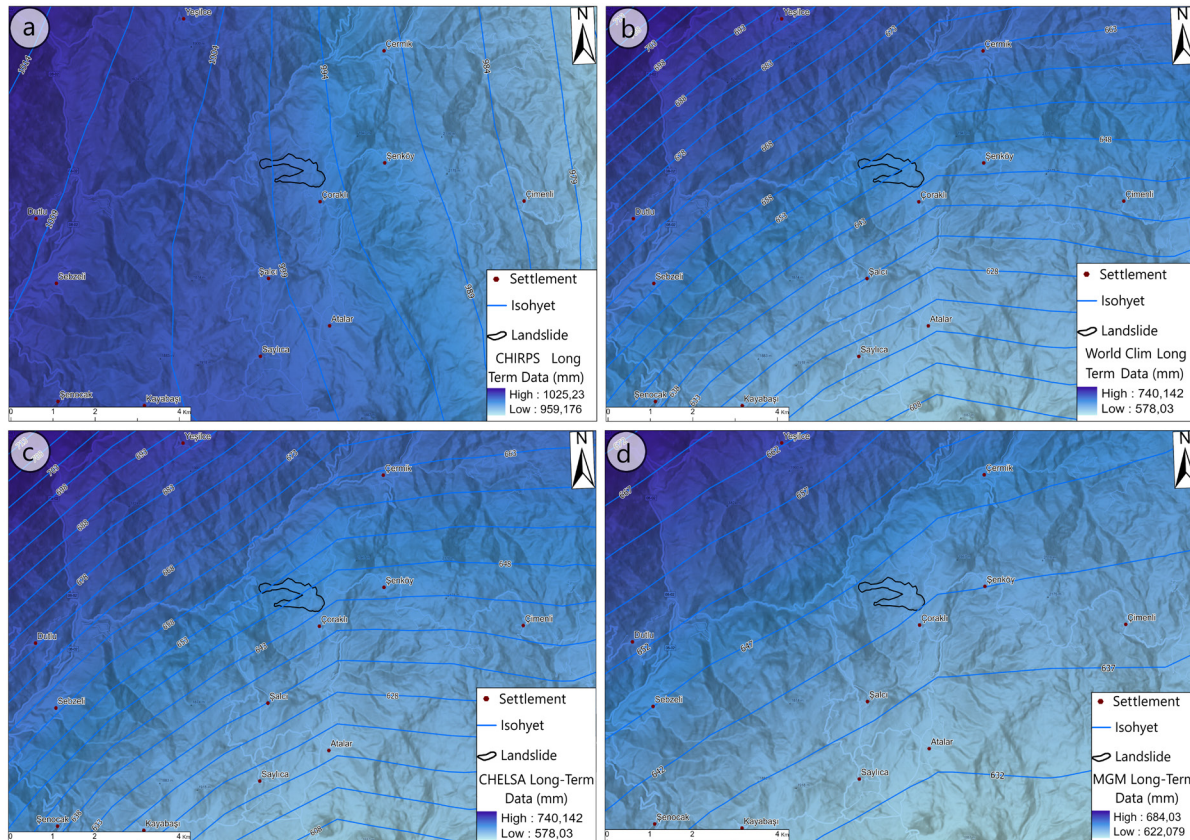

Figure 6. a. Distribution of precipitation according to CHIRPS data, b. Distribution of precipitation according to WorldClim data, c. Distribution of precipitation according to CHELSA data, d. Distribution of precipitation according to MGM data.
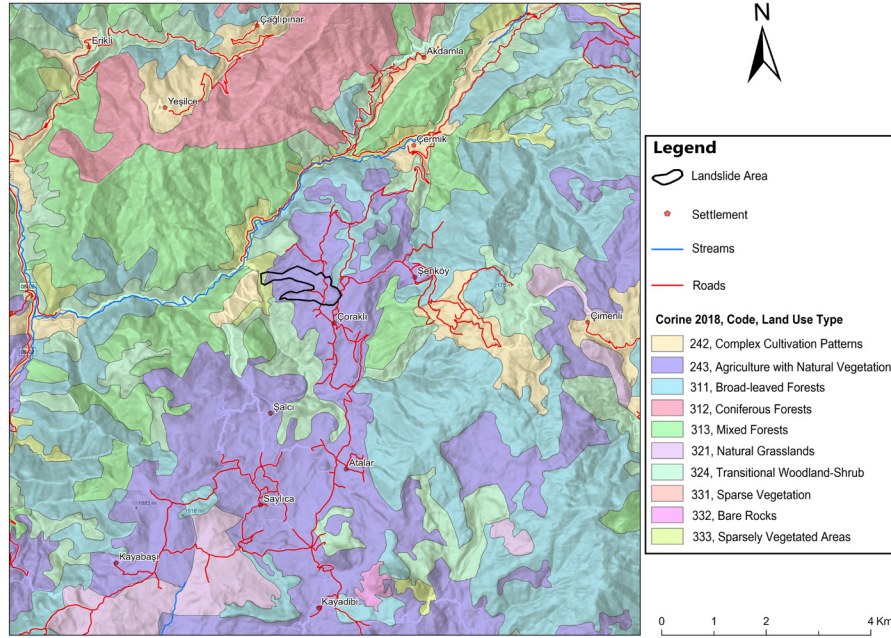
Figure 7. Land use in the study area and its vicinity according to Corine 2018 data.

of precision. According to the CHIRPS data, the landslide area receives precipitation ranging from 994-1000 mm (Figure 6 a), WorldClim data indicates 775-780 mm (Figure 6 b), CHELSA data shows 643-655 mm (Figure 6 c), and MGM data reveals 642-647 mm (Figure 6 d). When these interpolated data are evaluated together with meteorological station data to provide comparative features, it can be stated that the study area receives precipitation in the approximate range of 650-1000 mm. Another finding from the raster data was that precipitation values increased from southeast to northwest in the vicinity of the study area.

3.3. Land Use

Land use characteristics were assessed using Corine data which belong to 2018. Accordingly, the area where the Çoraklı landslide occurred generally exhibits land use characteristics dominated by natural vegetation and agricultural areas (Figure 7). Agricultural activities, plowing methods, and terracing can be related to erosion and landslides. Indeed, agricultural terracing in some parts of the study area has caused changes in the slope load balance. North of the slope where the landslide originated, there is a forested area composed of broad-leaved trees. To the east of the crown of the landslide, there are flat areas used for cultivated agriculture and pasture. From the front of the landslide scarp towards the deposition zone and within the deposition zone itself, sparse and short broad-leaved trees have developed. Within the study area, although there is a dense presence of trees in protected areas within valleys, the number of trees is lower on very steep and very gentle slopes. The

low vegetation density compared to the surroundings of the landslide area may be related to the young age of the landslide and the continuation of the shear flow movement (Figure 8). In other words, the short time spent for the development of the soil, which is the organism layer, and the vegetation on it may be effective. The scarcity of trees, especially in flat or gently sloping terrain, is a
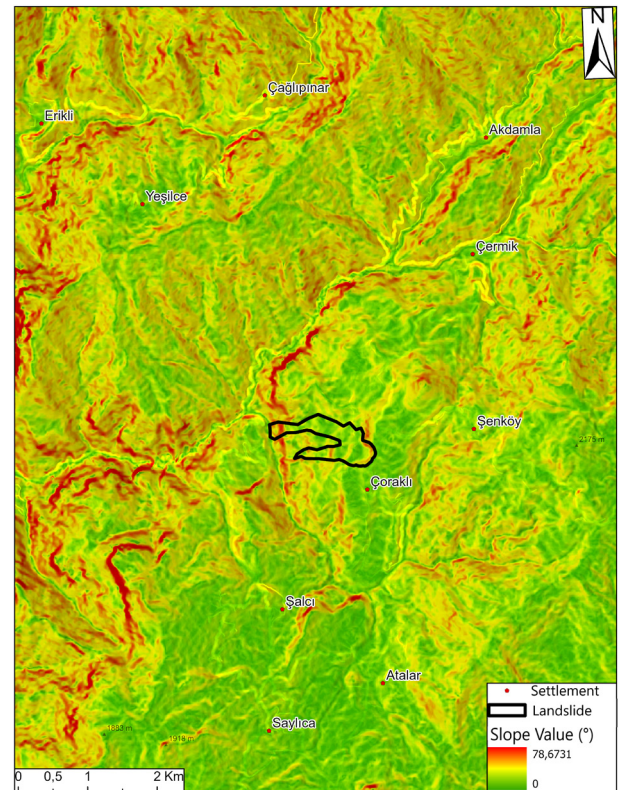

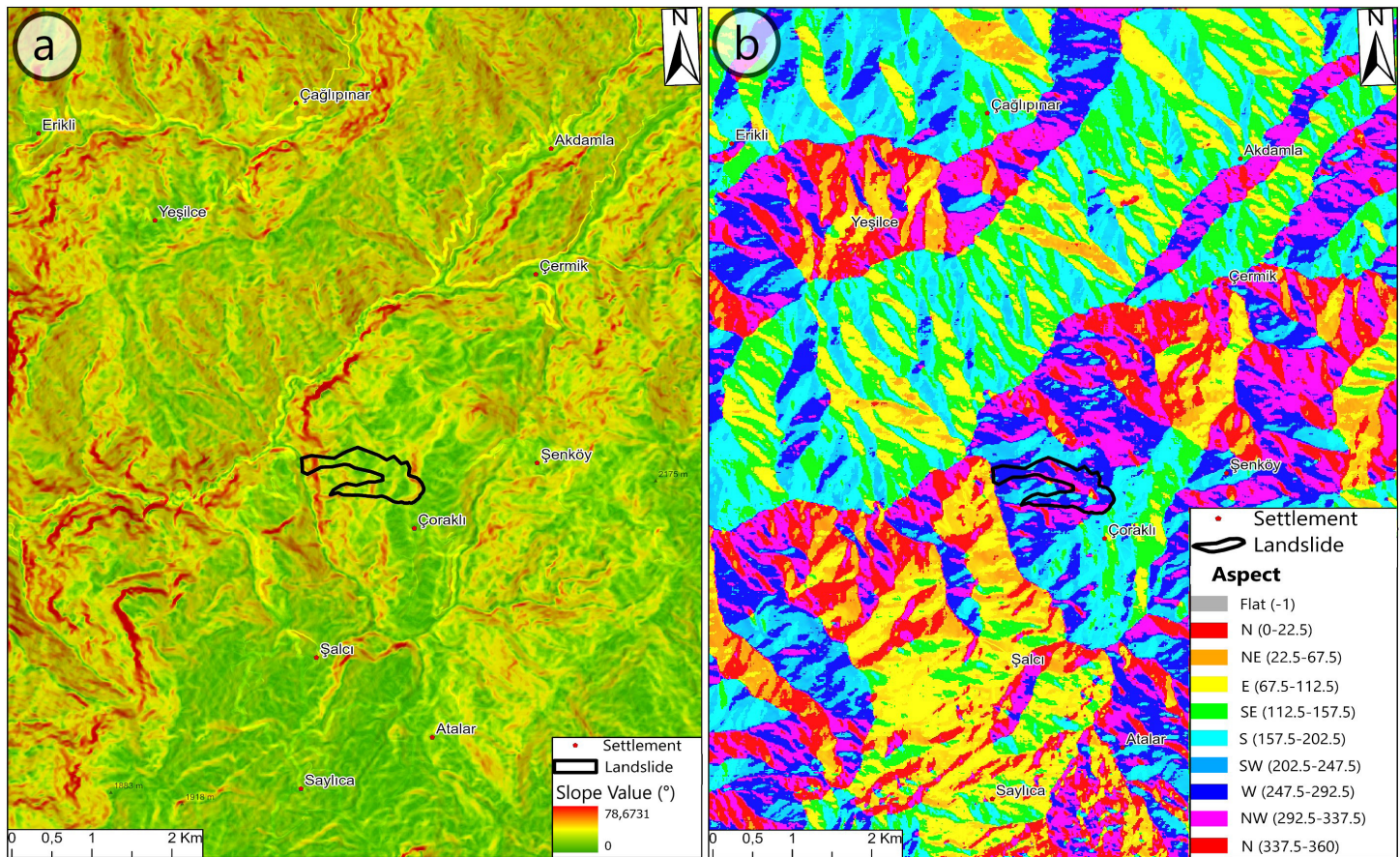**Figure 8:** NDVI map of the study area since 08/27/2024.

Figure 9. Slope map of the study area b. Aspect map of the study area.

significant indicator of human interventions on vegetation. Indeed, these areas are predominantly used for agricultural activities. Other elements of land use include the road passing 5-10 meters east of the landslide crown that connects villages and the roads traversing the landslide's material deposition area. These roads not only disrupt the stability of the slopes, but also increase the possibility of mass movements due to vibration and pressure caused by vehicles such as tractors, which travel rarely on these routes.

3.4. Morphometric Characteristics

Although the topography at the approximately 1700-meter elevation crown of the Çoraklı landslide, where the Çoraklı settlement center is also located, generally exhibits a plateau character, elevation differences exceeding 1000 meters within a few kilometers cause the topography to appear rugged.

On the slope where the landslide occurred, slope values were mostly >30°. The slope reaches particularly high values (ranging from 60° to 79°) in the area where the slopes begin from the valley floor. This is a result of rivers deeply incising their valleys and tectonic rejuvenation. These high slope values contribute to the destabilization of the upper slope. Another area with very high slope values was the landslide scarp, where the slope values exceeded 70° (Figure 9 a). These steep slopes have caused debris by the slope to fall into various parts of the landslide scarp and accumulate beneath the crown of the landslide.

The slopes in the area of the Çoraklı landslide are mostly oriented toward the west and northwest. The aspect conditions significantly influence the potential for the site to receive rainfall (Figure 9 b). In the study area, rainfall values increase progressively on the west-facing slopes and toward the northwest.

For the Çoraklı landslide area, a total of six topographic profiles were generated, with two oriented northwest-southeast and four oriented northeast-southwest. These topographic profiles reflect the very high slope values of the studied area. The results also reveal features such as the stepped appearance of the slope (Figure 10 A-A'), the concave curvature in the landslide scarp area, and the convex curvature in the deposition zone (Figure 10 X-X').
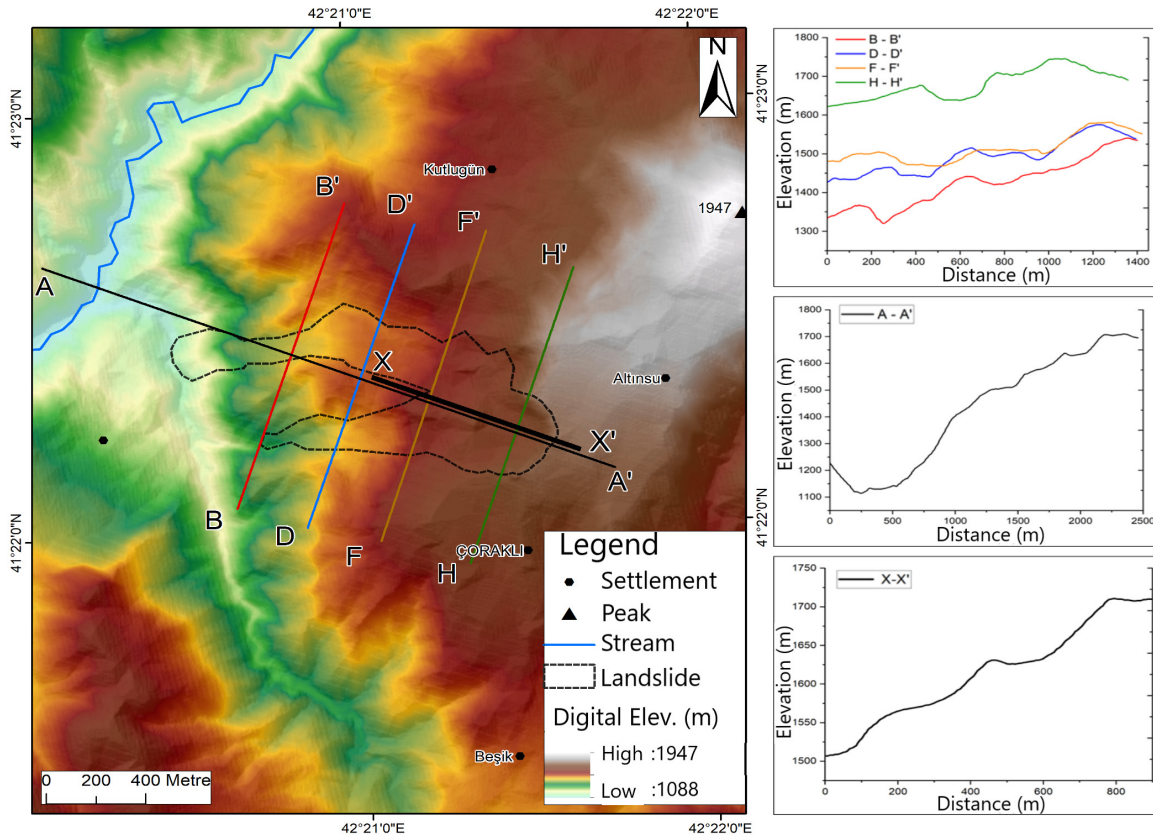
Figure 10. Topographic profile analysis.

As part of the study, longitudinal profiles were created for a total of nine streams, four of which flow through the landslide area and five through the surrounding area landslides, and their convexity ratios were calculated. The convexity factors of the longitudinal profiles for streams 1, 2, 3, and 4, which are located within the Çoraklı landslide area, were determined to be -11.63%, -24.12%, -17.78%, and -25.75%, respectively, indicating high convexity. Stream 5 (-10.70%) and Stream 9 (-5.92%) also indicate similar conditions. However, the values for Stream 6 (8.17%) and Stream 7 (7.96%) suggest moderate concavity. The value for Stream 8 (28.27%) indicates the most concave valley where the landslide occurred.

These calculated values indicate that the profiles of streams flowing through the Çoraklı landslide area to the northwest exhibit high convexity. The convex profile in the upper sections of these streams corresponds to the crown and scarp portions of the landslide, while the concave profile corresponds to a section that includes part of the slip zone and extends throughout the deposition zone down to the toe (Figure 11). In contrast, the profiles of streams flowing through surrounding area landslides generally exhibit concave characteristics throughout their course. This morphological difference suggests that the Çoraklı landslide is relatively younger compared to the surrounding area landslides,

where erosion and sediment redistribution appear to have progressed further.

The polygons drawn for the landslide and loss areas were analyzed using the PolyMorph-2D plugin (Figure 12). A 1/5,000 scaled DEM was used for drawing the polygons. The total landslide area assessed in this study was calculated to be 519,378.65 m², and the loss area was calculated as 98,369.48 m². The amount of material displaced in the landslide area was estimated at 6,718,732.8 m³, and in the loss area at 3,208,286 m³. The polygon length of the landslide area was measured at 5,299.084 m, and the bird's eye polygon length of the loss area was 1200.75 m (Table 1).

The W/L ratio was used to characterize the mass movement type. If the polygon is symmetrical and circular in appearance, the WTLR value is 1; for an elongated polygon, it approaches 0. There is a clear difference between the W/L ratios of flow-type and slide-type movements. Therefore, the W/L ratio is an acceptable index for determining the type of mass movement. In Sezer's 2010 study, the W/L ratios for debris flows ranged from 0.03 to 0.23, with an average value of 0.114. These ratios ranged from 0.23 to 2.83 for rotational slides. The maximum W/L range was obtained from single circular slide data, with maximum and minimum W/L values of 0.18 and 3.30, respectively. In the study area, the width-
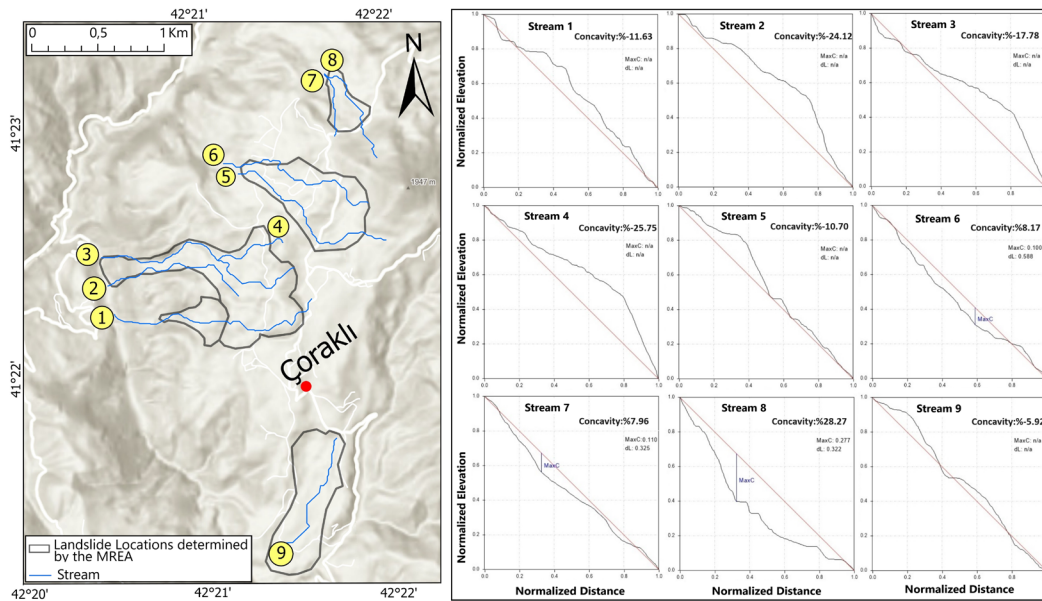
Figure 11. Longitudinal profiles of the rivers in the landslide area and surrounding area.

to-length ratio (W/L) (WTLR) was calculated as 0.421 for the landslide area and 0.79 for the loss area (Zingg, 1935). These values indicate flow movement in the landslide area.

The Ellipticity Factor (L_W)/(L+W) (ELLF) (Buendía et al., 2002) equals zero for polygons resembling a perfectly symmetrical circle on all axes, while in elongated polygons, the ellipticity value approaches 1 (Güler et al., 2021). The ellipticity values were determined as 0.408 for the landslide area and 0.12 for the loss area. The departure of the ellipticity value from zero indicates elongated axes in the landslide area. This situation in the field was attributed to the flow of landslide material into river valleys.

Long-term rock avalanches or soil flows typically have thin-layers. These features are also applicable to weak rock or soil slides. In such cases, multiple landslides and debris sources spreading in different directions, which cannot be represented by a simple maximum-length calculation, should be considered. Therefore, the perimeter of the main outline was used as the basic parameter to calculate the elongation factor (Havenith, 2015). The Elongation Factor (ELOF) (Schumm, 1956) was calculated in this study. The shape of a polygon can be described by the elongation factor (ELOF), which is the ratio of the diameter of a circle to the length of the polygon. The ELOF value is 1 for a perfectly circular polygon and 0 for a long and narrow polygon. The ELOF indicates how circular or elongated the polygon is (Güler et al., 2021). Debris flows and rock avalanches generally have a high elongation factor. Subsidence and compact rock slides (small areal) may have an elongation

factor >0.8 (Havenith et al., 2015). In this study, an elongation factor of 0.512 was identified in the landslide area, while a value of 0.91 was determined for the loss area (Table 1). These values indicate a relatively high elongation factor in the general landslide area due to flow movement and a low elongation factor in the loss area due to sliding and subsidence.

The concave slope sections have more soil thickness and groundwater concentration than the convex sections. As a result, during and after rainfall, soil on concave slopes is more likely to become saturated, increasing the likelihood of soil slippage. Concave slopes are areas where landslides and surface flows occur most frequently. On the other hand, mass movements, such as rockfalls, typically occur on highly steep convex slopes (Massari & Atkinson, 1999).

For the study area, the 2D polygonal Convexity factor was calculated. The formula for convexity is CONV (PCHU /P) (CONC) (Glasbey and Horgan, 1995), which provides information about the general roughness of a polygon's boundary and is not affected by the overall shape of the polygon. If a polygon's boundary lacks concave regions, it is considered convex. The convexity is calculated by a geometric shape known as a convex hull (CHU). The convexity measure can be expressed as the ratio between the perimeter of the convex hull (PCHU) and the actual polygon perimeter (PPOL). The more irregular the polygon, the more it differs from the convex hull (CHU). The CONV value of a smoothly bounded convex polygon is close to 1, while that of an irregularly bounded polygon is close to 0 (Glasbey & Horgan, 1995; Güler et al., 2021). Because of the
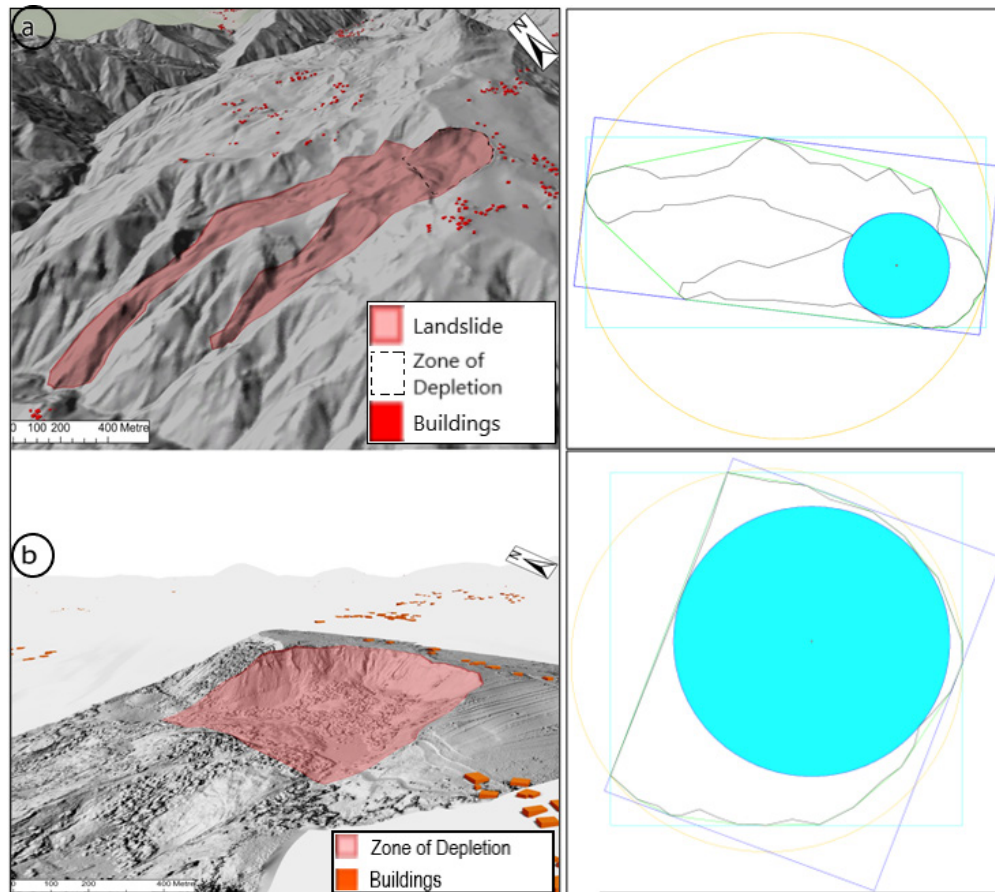
Figure 12. Polygons analyzed using the PolyMorph-2D plugin: A. Landslide Area, B. Depletion Zone.

Table 1. *2D and 3D Polygonal Measurements.*

Parameter	Landslide Area	Zone of Depletion	
Polygon Area (m²)	519378,65	98369,48	
Amount of Moving Material (m³)	6718732,8	3208286	
Polygon Aerial Length (PPOL)	5299,084	1200,75	
Major Axis Length (LPOL) (L)	1588,186	388,43	
Minor Axis Length (WPOL) (W)	668,419	308,3	Güler vd., 2021
Angle from North to East (0°-179°)	96,936	20,71	
Minimum Bounding Box Area within the Polygon (AMEB)	1061573,476	119751,86	
Convex Hull Area	805464,93	100067,88	
Minimum Circumscribed Circle Radius within the Polygon (RMCC)	798,915	209,27	
Largest Inscribed Circle Area within the Polygon (AMIC)	133538,463	68289,09	
Width-to-Length Ratio (W/L) (WTLR)	0,421	0,79	Zingg (1935)
Ellipticity Factor (L-W)/(L+W) (ELLF)	0,408	0,12	Buendía et al. (2002)
Elongation Factor (4A/π)0.5 / L (ELOF)	0,512	0,91	Schumm (1956)
Polygon Area (m²)	0,701	0,99	Glasbey & Horgan (1995)

analysis, the convexity values were 0.701 in the landslide area and 0.99 in the loss area (Table 1). These values indicate high convexity. As seen in the elevation and stream profiles, the overall curvature of the slope is convex.

In landslide hazard assessments, it is important to analyze slopes in detail. Adjacent slopes with the same lithology may receive different hazard ratings based on differences in the slope angle and land use, among other factors. Even within a single land unit, distinctions should be made between different slope sections. For example, a concave slope should be evaluated differently from an adjacent flat or convex slope when necessary. This detailed examination helps to assign a hazard rating based on the unique characteristics of each slope section (Soeters & Westen, 1996). High-resolution topographic data reveal numerous convex and concave transitions in the study area. These small concave-convex topographic transitions in the
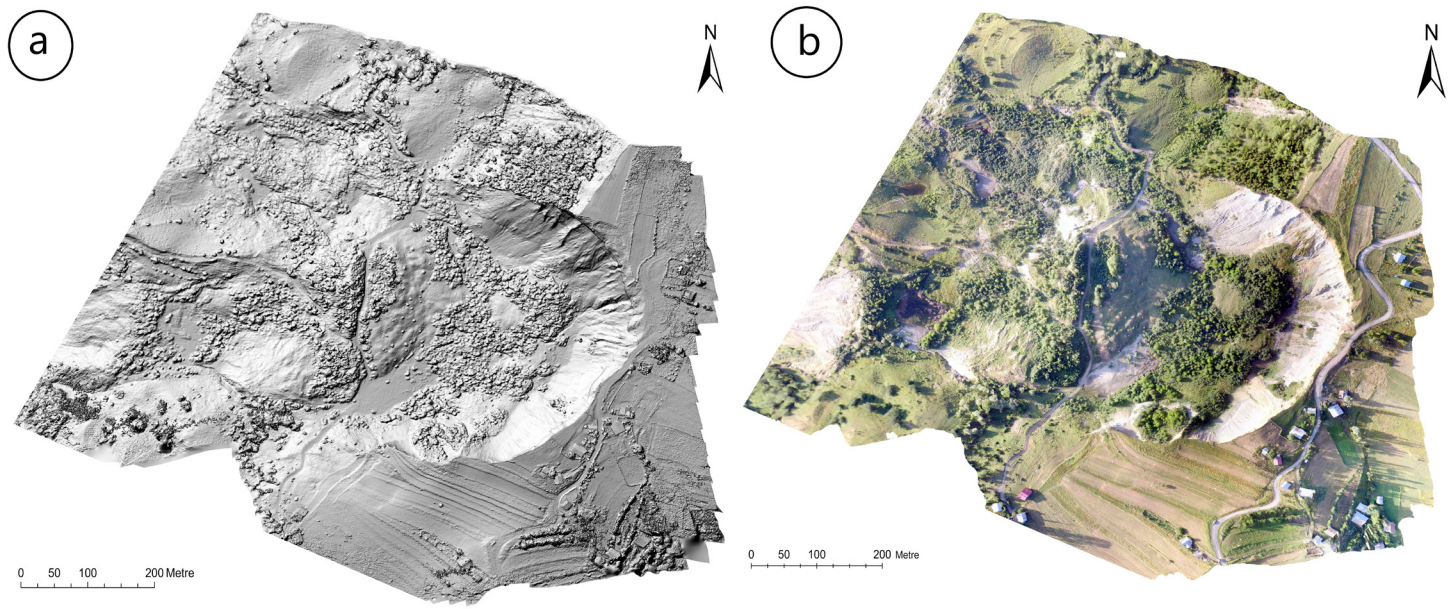
Figure 13. a. Hillshade image of the landslide area. b. Orthophoto of the landslide area.

landslide area cause surface water to accumulate in depressions or pass through finer soils. Depending on factors such as slope, soil material, and amount of water present, this can lead to ground instability.
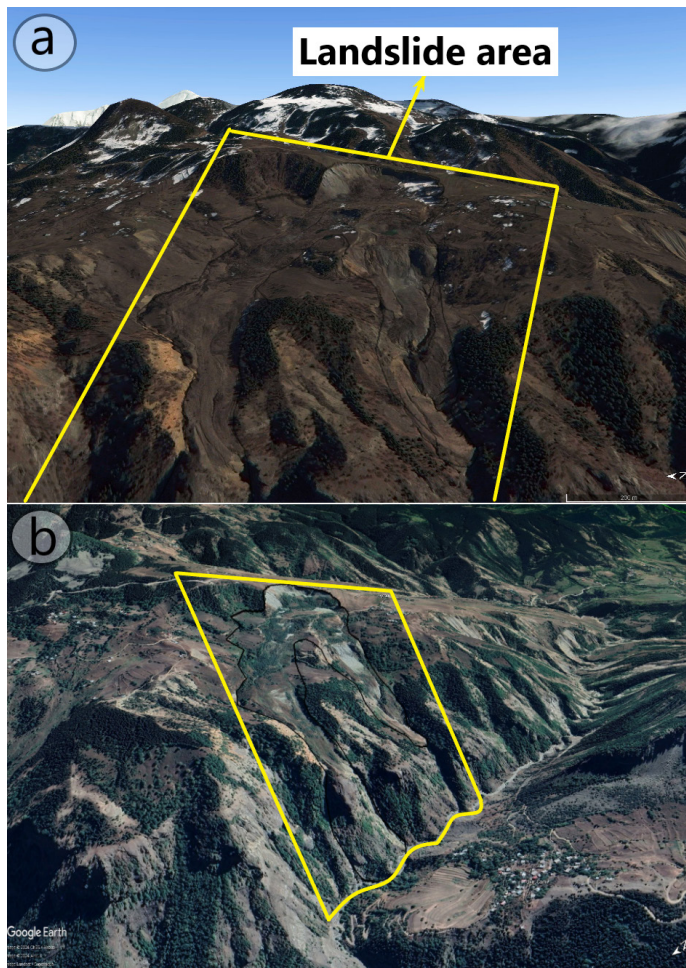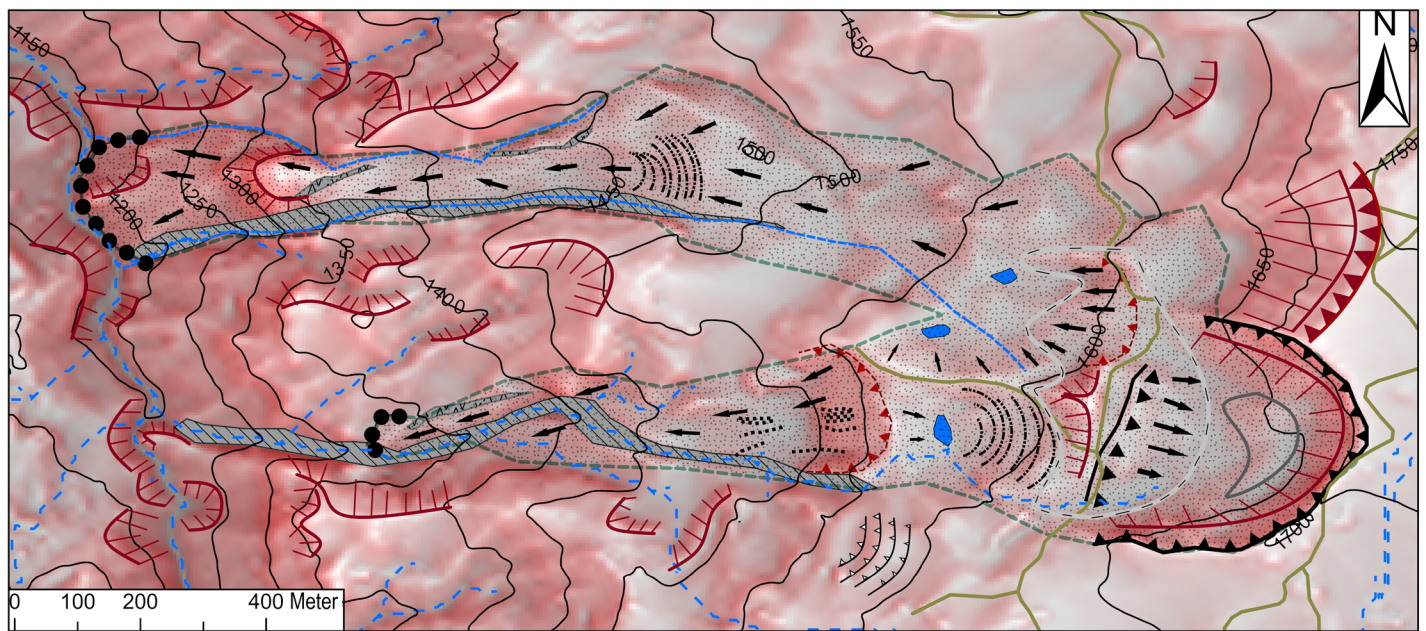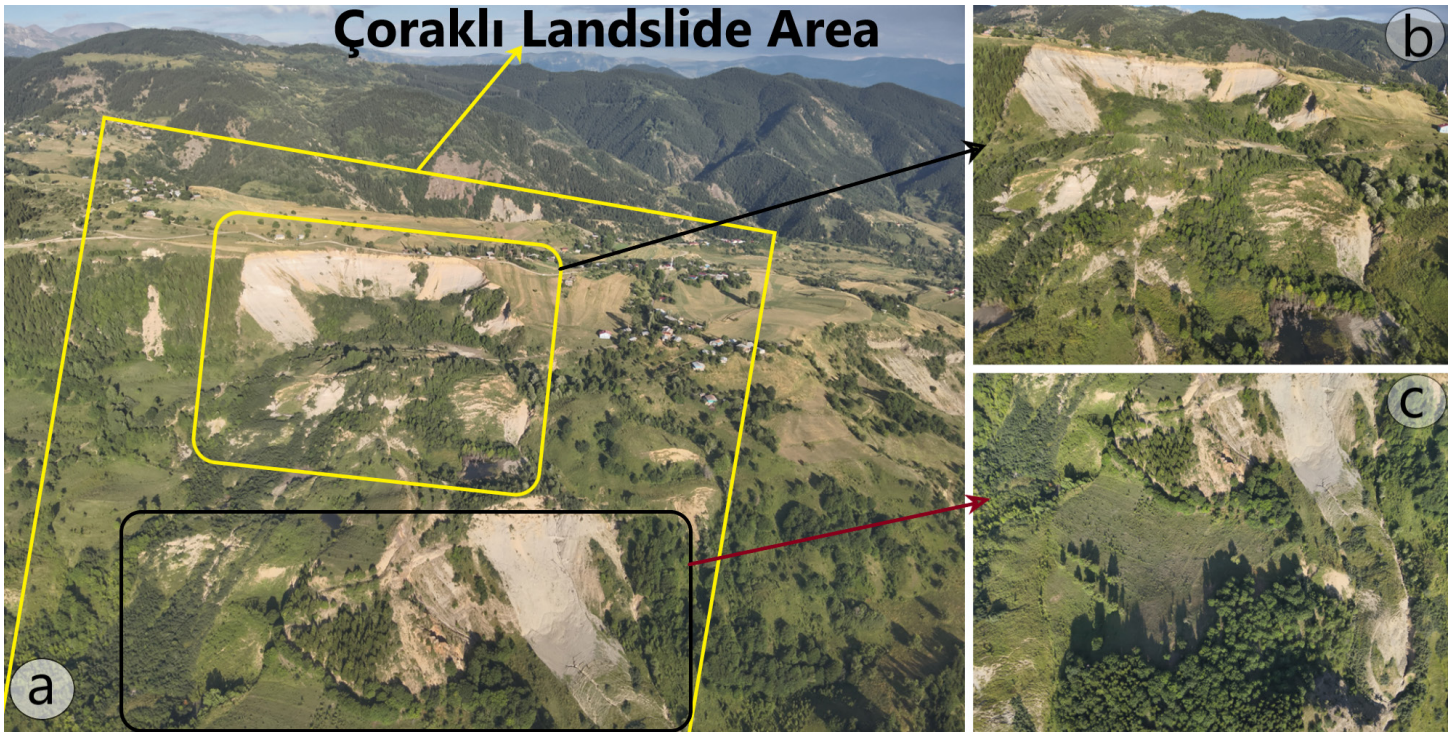
3.5. Geomorphological Features

The landslide, which began as a slide at an elevation range of 1170-1700 meters, transitioned into a debris flow as it moved toward the valley floor. A distinct crescent-shaped main landslide scarp, approximately 60 meters in height, formed as a result of the landslide (Figure 13 a). The longest part of the distance between the right and left wings was 345 m, and the long axis of the landslide body was about 500 m. The closest point between the road that connects the center of Çoraklı village to the northern villages and neighborhoods and the landslide's crown is less than 5 m, and the distance between the residential structures and the landslide's crown falls below 20 m in some places (Figure 13 b). These parameters were calculated from DEM which produced by a UAV.

It has also been observed that there is mass movement in the form of sliding and very recent flow from the crown of the main landslide toward the west. The seasonal streams and gullies formed by flash floods on this loose material are likely to destabilize the slopes and landslide debris in the surrounding area. Additionally, the increasing slope toward the western valley reaches very high values, facilitating the flow of material. Snowmelt also plays a role in triggering material flow. The lack of vegetation development in this area indicates that the flow movement was relatively recent. In the south of the landslide area and in the nearby sections, small-scale step-like structures,

Figure 14. Google Earth images of the landslide area.

Photo 2. a. Flow movement starting from the deposition zone of the Çoraklı landslide scarp. b. Stepped structures resembling rotational sliding where slope stability is compromised. Flow traces where the slope increases.

Legend

Gully Erosion	Main scarp	Ephemeral stream	Current cracks and movement direction	i-value	
Secondary Scarps	Landslide Area	Steep slopes	Flow direction	0,416631	
Head of the Flow Slope	Flow-induced scarp	Ancient landslide scarp	Lake	-0,471951	
Anti-slope direction	Gully steepness	Depositional zone of slide material 1	Road		
Toe		Depositional zone of slide material 2	Contour		

Figure 15. Geomorphological map of the landslide area.

indicative of sliding, and secondary cracks are noticeable in areas where slope stability has weakened, from the valley floor toward Çoraklı village (Figure 14 a-b; Photo 2-a, b, c).

In the Çoraklı landslide, which began with a slide from approximately 1700 m toward the west, the accumulation of the sliding material in front of the landslide scarp occurred in two zones at an elevation range of 1600–1630 m. From this point toward the west, as the elevation decreases from 1620 m to 1550 m, the sliding movement gradually transitions into a flow of material. From this point onwards, the material, now moving in a flow pattern, integrated into the pre-existing river valleys in the area and moved toward the western valley in two branches. In the landslide area and its vicinity, steep topography slopes, the juxtaposition of concave and convex structures, and undulating, sloped surfaces have led to the formation of numerous lakes. The cracks and step-like structures formed by sliding and flow in and around the landslide area indicate ongoing movement from the toe to the crown of the landslide (Figure 15). Just north of the landslide area, there is a site resembling a landslide scarp but with well-developed vegetation, indicating that it is an older landslide site than the studied area. Although there are numerous landslide sites of varying sizes around the Çoraklı settlement, the youngest of these is the Çoraklı landslide.

4. DISCUSSION

Çoraklı landslide provides an important case study to understand the effects of geomorphological and topographic factors on landslide susceptibility. Landslides in the immediate vicinity generally occurred with similar geomorphological effects and mechanisms. The landslide, beginning from elevations of approximately 1700 meters and transitioning to a debris flow, highlights the intricate relationship between elevation, slope dynamics, and material movement. The accumulation of sliding material in two distinct zones between elevations of 1600 m and 1630 m, followed by a transition to flow behavior at lower elevations, emphasizes the complex processes involved in landslide evolution.

The integration of material flow into pre-existing river valleys and the formation of branching flow paths toward the western valley further illustrate the dynamic nature of the landslide. The steep, concave, and convex topographic features within and around the landslide area have contributed to the development of numerous small lakes and have impacted slope stability. The presence of cracks and step-like structures across the landslide area indicates ongoing movement and instability,

with a clear differentiation between recent and older landslide features in the vicinity.

The landslide area north of Çoraklı, characterized by well-developed vegetation, serves as a reference for older landslide features compared to the active Çoraklı landslide. This comparison underscores the relative youth of the Çoraklı landslide and suggests the progression of landslide activity in the region. Despite the presence of numerous landslides of varying sizes around Çoraklı, the Çoraklı landslide was identified as the most recent, highlighting its significance in current hazard assessments.

In general, villages and settlements established on slopes or hills with high clay content, coupled with roads traversing areas of slope instability, are increasingly susceptible to landslides due to seasonal rainfall. This susceptibility is exacerbated by accumulating material on steep slopes and the development of concave and convex topographic features, which significantly enhance landslide risk. The stream continuously eroded the heel of the Çoraklı landslide and played a role in slope instability. In this case, the risk is significantly increased.

The findings of this study suggest that areas with high clay content and disturbed slope stability are particularly vulnerable to landslides. Seasonal rainfall further intensifies these risks, leading to significant increases in landslide susceptibility. The ongoing movement and instability observed in the Çoraklı landslide area along with the formation of new features such as lakes and cracks underscore the need for continuous monitoring and risk assessment to mitigate the impacts of landslides in similar environments.

The detailed analysis of slope morphology, material flow patterns, and topographic features provides valuable insights into the processes driving landslide activity. By understanding these factors, we can better predict and manage landslide risks, particularly in regions where natural and human-induced factors contribute to slope instability. Future research should focus on enhancing early warning systems and developing targeted mitigation loss strategies to address the challenges of landslides in vulnerable areas.

5. CONCLUSION

In a location very close to the settlement area in the northwest of Çoraklı village, Şavşat district, Artvin province, a landslide that initially occurred as a slippage starting from an elevation of 1700 meters has formed a crescent-shaped landslide scarp approximately 60 meters high. The landslide, which started as a

slip, continued as a flow movement in previously established river valleys on a young convex slope. The toe of the landslide ended in the western river valley.

Although varied across the slope, high slope values, aspect factors leading to a relative increase in precipitation, intense snowfall, and snowmelt, in addition to the presence of different lithological units with high clay production potential at the contact zone, were the main factors triggering the landslide. Human interventions such as land-use changes and agricultural expansion can disrupt slope stability. Vibrations caused by vehicles passing near the landslide crown and through the landslide loss zone may destabilize the slope and trigger further movement.

The freshness of the flow-type mass movements, secondary stepped structures, ponding, and lack of vegetation on the flow material indicate that the area is an active landslide site. Along with the active nature of the Çoraklı landslide site, the presence of other older landslides indicates that the area is highly sensitive to mass movements. Therefore, relocation of residences and other settlement units very close to the landslide area in Çoraklı to safer locations. Furthermore, reassessment of land use in the region and limitation of construction in high-landslide-risk areas are crucial steps to mitigate the effects of future mass movements. In the long term, these measures can enhance the safety of settlement areas, protect public health, and reduce economic losses.

REFERENCES

Alimohammadlou, Y., Najafi, A., & Yalcin, A., (2013). Landslide process and impacts: A proposed classification method, CATENA, (104), 219-232, https://doi.org/10.1016/j.catena.2012.11.013.

Amarasinghe, M. P., Kulathilaka, S. A. S., Robert, D. J., Zhou, A., & Jayathissa, H. A. G. (2024) Risk assessment and management of rainfall-induced landslides in tropical regions: a review. Nat Hazards 120, 2179–2231. https://doi.org/10.1007/s11069-023-06277-3

Aykır, D. (2023). Yol boyu heyelanlarına bir örnek: Ardahan-Göle Heyelanı. Jeomorfolojik Araştırmalar Dergisi (11), 52-70. https://doi.org/10.46453/jader.1288368

Bayrakdar, C., Görüm, T., Çılğın, Z., Vockenhuber, C., Ivy-Ochs, S. & Akçar, N. (2020) Chronology and Geomorphological Activity of the Akdag Rock Avalanche (SW Turkey). Front. Earth Sci. 8:295. doi: 10.3389/feart.2020.00295.

Bozdoğan, M., & Canpolat, E. (2022). Analitik Hiyerarşi Süreci (AHS) İle Delibekirli (Kırıkhan/Hatay) Havzası'nın Kütle Hareketleri Duyarlılık Analizi. Ege Coğrafya Dergisi, 31(1), 33-53. https://doi.org/10.51800/ecd.1054815.

Buendía, P., Soler, C., Paolicchi, F., Gago, G., Urquieta, B., Pérez-Sánchez, F., & Bustos-Obregón, E., (2002). Morphometric characterization and classification of alpaca sperm heads using the Sperm-Class Analyzer® computer-assisted system. Theriogenology, (57), no. 4, 1207–1218. https://doi.org/10.1016/s0093-691x(01)00724-5

Canpolat, E., (2021). Kırmızı relief görseli analizi (red relief ımage analysis-rrim) ve erişilebilir sayısal yükselti modeli (dem-sym) verilerinin karşılaştırılması, Mehmet Fatih Döker, Ebru Akköprü (Eds.), Coğrafi Bilgi Sistemleri Uygulamalari II kitabı içinde (s. 251-269), Ankara: Pegem Akademi.

Chiba, T., Kaneta, S. I., & Suzuki, Y. (2008). Red relief image map: new visualization method for three-dimensional data. *Int Arch Photogramm Remote Sens Spac Inform Sci*, 37(B2), 1071-1076.

Cihangir, M. E., Görüm, T., & Nefeslioğlu, H. A. (2018). Heyelan tetikleyici faktörlerine bağlı mekânsal hassasiyet değerlendirmesi. Türk Coğrafya Dergisi(70), 133-142. https://doi.org/10.17211/tcd.410998.

Corine, (2018). Europe, 6-yearly–version. Retrieved fromhttps://doi.org/10.2909/71c95a07-e296-44fc-b22b-415f42acfdf0

Cruden, D. M., & Varnes, D. J., (1996). Landslide types and processes. Landslides investigation and mitigation, Special Report 247. In: Turner, A.K. and Schuster, R.L. (eds.), 36–75.

Dai, F. C., Lee, C. F., & Ngai, Y. Y. (2002). "Landslide risk assessment and management: An overview." Engineering Geology, 64(1), 65-87.

Doğu, A. F., Çiçek, İ. ve Gürgen, G. (1989) 23 Haziran 1988 Çatak Heyelanı (Trabzon-Maçka). Atatürk Dil ve Tarih Yüksek Kurumu, Coğrafya Araştırmaları, 1(1), 103-109.

Duman, T. Y., Olgun, Ş., Çan T., Nefeslioğlu, H. A., Hamzaçebi, S., Elmacı, H., Durmaz, S., & Çörekçioğlu, Ş. (2009). Türkiye Heyelan Envanteri Haritası 1/500.000 Ölçekli Kars Paftası.

Eker, R., Aydın, A. & Görüm, T. (2024). Tracking deformation velocity via PSI and SBAS as a sign of landslide failure: An open-pit mine-induced landslide in Himmetoğlu (Bolu, NW Turkey). Nat Hazards 120, 7701–7724. https://doi.org/10.1007/s11069-024-06533-0

EM-DAT, CRED/UCLouvain, (2024). 2023 Disasters in numbers. https://files.emdat.be/reports/2023_EMDAT_report.pdf

Erginal, A.E., Türkeş, M., Ertek, T.A., Baba, A. & Bayrakdar, C. (2008) Geomorphological investigation of the excavation-inducedDündar landslide, Bursa – Turkey. Geogr. Ann., 90 A (2): 109–123.

Erginal, E. A. ve Bayrakdar, C. (2005). Karayolu Heyelanına bir örnek: İnecik Heyelanı (Tekirdağ), İstanbul Coğrafya Dergisi, 14, 43-53. https://dergipark.org.tr/tr/pub/iucografya/issue/25063/264592

Erinç, S., (2002). Jeomorfoloji I (6. b.). İstanbul: Der Yayınları.

Ertek, A. (1999). Kandıra-Arıklar Heyelanı (20 Ekim 1997). İstanbul Üniversitesi Edebiyat Fakültesi Coğrafya Bölümü Coğrafya Dergisi, 7, 87-103.

Fick, S. E., & Hijmans, R. J., (2017). WorldClim 2: new 1-km spatial resolution climate surfaces for global land areas. International Journal of Climatology, 37(12), 4302–4315. doi:10.1002/joc.5086.

Fidan, S., & Görüm, T. (2020). Türkiye'de ölümcül heyelanların dağılım karakteristikleri ve ulusal ölçekte öncelikli alanların belirlenmesi. Türk Coğrafya Dergisi(74), 123-134.

Fidan, S., Tanyaş, H., Akbaş, A., Lombardo, L., Petley, D. N., and Görüm, T. (2024). Understanding fatal landslides at global scales: a summary of topographic, climatic, and anthropogenic perspectives. Natural Hazards, 1-19. 120:6437–6455 https://doi.org/10.1007/s11069-024-06487-3

Funk, C., Peterson, P., Landsfeld, M., Pedreros, D., Verdin, J., Shukla, S., ... & Michaelsen, J. (2015). Climate hazards infrared precipitation with stations—a new environmental record for monitoring extremes. Scientific data, 2(1), 1-21.

Glasbey, C.A., & Horgan, G.W., (1995). Image Analysis for the Biological Sciences. John Wiley & Sons, Chichester.

Gökçe, O., Özden, Ş., ve Demir, A. (2008). Türkiye'de afetlerin mekânsal ve istatistiksel dağılımı afet bilgileri envanteri. Bayındırlık ve İskan Bakanlığı Afet İşleri Genel Müdürlüğü.

Görüm, T., & Fidan, S., (2021). Spatiotemporal variations of fatal landslides in Turkey. Landslides 18, 1691–1705 https://doi.org/10.1007/s10346-020-01580-7.

Görüm, T., Tanyas, H., Karabacak, F., Yılmaz, A., Girgin, S., Allstadt, K. E., ... & Burgi, P. (2023). Preliminary documentation of coseismic ground failure triggered by the February 6, 2023 Türkiye earthquake sequence. Engineering Geology, 327, 107315.

Gutiérrez, F., & Gutiérrez, M. (2016). Slope Movements. Landforms of the Earth: An Illustrated Guide, 127-154. https://doi.org/10.1007/978-3-319-26947-4_8 8

Güler, C., Beyhan, B., & Tağa, H. (2021). PolyMorph-2D: An open-source GIS plug-in for morphometric analysis of vector-based 2D polygon features. Geomorphology, 386, 107755. https://doi.org/10.1016/j.geomorph.2021.107755.

Havenith, H. B., Strom, A., Torgoev, I., Torgoev, A., Lamair, L., Ischuk, A., & Abdrakhmatov, K., (2015). Tien Shan Geohazards Database: Earthquakes and landslides, Geomorphology, 249, 16-31, https://doi.org/10.1016/j.geomorph.2015.01.037.

Karger, D. N., Conrad, O., Böhner, J., Kawohl, T., Kreft, H., Soria-Auza, R. W., ... & Kessler, M. (2017). Climatologies at high resolution for the earth's land surface areas. Scientific data, 4(1), 1-20. https://doi.org/10.1038/sdata.2017.122.

Kopar, İ. (2011). Oluşmuş ve aktivitesini sürdüren karışık tip bir heyelan: Elmalı-Madenköprübaşı (İspir-Erzurum) Heyelanı, sorunlar ve öneriler. Doğu Coğrafya Dergisi, 15(24), 191-209.

Makonyo, M., & Zahor, Z. (2023) GIS-based analysis of landslides susceptibility mapping: a case study of Lushoto district, north-eastern Tanzania. Nat Hazards 118, 1085–1115. https://doi.org/10.1007/s11069-023-06038-2.

Massari, R., & Atkinson, P. M. (1999). Modeling susceptibility to landsliding: An approach based on individual landslide type. Transactions of the Japanese Geomorphological Union, 20, 151-68.

Moazzam, M.F.U., Vansarochana, A., Boonyanuphap, J., Sittichai, C., Ghani, R., Geraud Poueme, D. (2020) Spatio-statistical comparative approaches for landslide susceptibility modeling: case of Mae Phun, Uttaradit Province, Thailand. SN Appl. Sci. 2, 384. https://doi.org/10.1007/s42452-020-2106-8

MTA (2010). Artvin Maden ve Enerji Kaynakları, https://www.mta.gov.tr/v3.0/sayfalar/ bilgi-merkezi/maden_potansiyel_2010/Artvin_Madenler.pdf.

MTA Jeoloji Haritası: 1/100000 Ölçekli-Pafta No: Ardahan F48.

MTA, (1998). Artvin İlinin Çevre Jeolojisi ve Doğal Kaynakları, MTA Raporları, Rapor No: 10165, Jeoloji Etütleri Dairesi Başkanlığı, Ankara.

Niraj, K.C., Singh, A. & Shukla, D.P. (2023) Effect of the Normalized Difference Vegetation Index (NDVI) on GIS-Enabled Bivariate and Multivariate Statistical Models for Landslide Susceptibility Mapping. J Indian Soc Remote Sens 51, 1739–1756. https://doi.org/10.1007/s12524-023-01738-5

Özpolat, E., Yıldırım, C., & Görüm, T., (2020). The Quaternary landforms of the Büyük Menderes Graben System: the southern Menderes Massif, western Anatolia, Turkey. Journal of Maps, 16(2), 405-419. https://doi.org/10.1080/17445647.2020.1764874.

Pérez-Peña, J. V., Al-Awabdeh, M., Azañón, J. M., Galve, J. P., Booth-Rea, G., & Notti, D., (2017). SwathProfiler and NProfiler: Two new ArcGIS Add-ins for the automatic extraction of swath and normalized river profiles. Computers & Geosciences, 104(135), 150. https://doi.org/10.1016/j.cageo.2016.08.008.

Reis, S., Bayrak, T., Yalçın, A., Atasoy, M., Nişancı, R., and Ekercin, S. (2008). Rize Bölgesinde Yağış Heyelan Ilişkisi. Jeodezi ve Jeoinformasyon Dergisi, (99), 5-9. Schumm, S. A. (1956). Evolution of drainage systems and slopes in badlands at Perth Amboy, New Jersey. Geological society of America bulletin, 67(5), 597-646.

Schuster, R.L., & Highland, L. M. (2007). The Third Hans Cloos Lecture. Urban landslides: socioeconomic impacts and overview of mitigative strategies. Bull Eng Geol Environ 66, 1–27. https://doi.org/10.1007/s10064-006-0080-z

Sellers, P. J., (1985). "Canopy reflectance, photosynthesis and transpiration." International Journal of Remote Sensing, 6(8), 1335-1372. doi:10.1080/01431168508948283

Sezer, E., (2010). A computer program for fractal dimension (FRACEK) with application on type of mass movement characterization. Computers & Geosciences, 36, (3), 391-396, https://doi.org/10.1016/j.cageo.2009.04.006.

Soeters, R. & Westen, C. J. Van, (1996). "Slope Instability Recognition, Analysis and Zonation," In: A. K. Turner & R. L. Schuster, (Eds.), Landslides: Investigation and Mitigation: Sp. Rep. 247 (pp. 129-177)., Transportation Research Board, National research Council, National Academy Press, Washington DC.

Tarım ve Orman Bakanlığı, (2024). CORINE arazi örtüsü bilgi notu. http://corine.ormansu.gov.trcorineportal/araziortususiniflari.html adresinden alınmıştır.

Taşdemiroğlu, M. (1970). Türkiyede kütle hareketleri. Türkiye Jeoloji Bült. 13(2), 26-35.

Tucker, C.J., (1979). "Red and photographic infrared linear combinations for monitoring vegetation." Remote Sensing of Environment, 8(2), 127-150. doi:10.1016/0034-4257(79)90013-0

Varnes, D. J., (1978), Slope movement types and processes. In: Schuster R. L. & Krizek R. J. (Ed.), Landslides, analysis and control (pp. 11–33.). Transportation Research Board Sp. Rep. No. 176, Nat. Acad. oi Sciences,

Varnes, D. J., (1984). Landslide hazard zonation: A review of principles and practice. Commission of landslides of the IAEG, UNESCO", Natural Hazards, 3, 61.

WP/WLI (Working Party on World Landslide Inventory), (1993). A suggested method for describing the activity of a landslide, IAEG Bull. 47, 53-57.

Xia, L., Shen, J., Zhang, T., Dang, G., & Wang, T. (2023). GIS-based landslide susceptibility modeling using data mining techniques. Frontiers in Earth Science, 11, 1187384. doi: 10.3389/feart.2023.1187384.

Yılmaz B. S., Gülibrahimoğlu, İ., Konak, O., Yazıcı, E. N., Köse, Z., Yaprak, S., Çuvalcı, F., Saraloğlu, A., ve Tosun, C. Y., (1998). Artvin ilinin çevre jeolojisi ve doğal kaynakları, MTA Genel Müdürlüğü Jeoloji Etütleri Dairesi, Ankara.

Zingg, T., (1935). Beitrag zur Schotteranalyse. Schweizerische Mineralogische und Petrographische Mitteilungen, 15, (1), 39–140.